

Microstructure and Field Angle Dependence of Critical Current Densities in REBa₂Cu₃O_y Thin Films Prepared by PLD Method

Y. Ichino, R. Honda, M. Miura, M. Itoh, Y. Yoshida, Y. Takai, K. Matsumoto, M. Mukaida, A. Ichinose, and S. Horii

Abstract—A *c*-axis oriented epitaxial REBa₂Cu₃O_y (RE123) thin film performs excellent superconducting properties in magnetic field. Recently, we reported that a critical current density (J_c) in the RE123 thin film was improved by a deliberate composition control. A Sm_{1+x}Ba_{2-x}Cu₃O_y (Sm123) thin film with a small amount of Sm/Ba substitution x showed the great $J_c \sim 0.17$ MA/cm² in 5 T at 77.3 K, while the J_c in (Yb_{1-z}Nd_z)Ba₂Cu₃O_y (Yb/Nd123) thin films depended on an amount of mixed crystal ratio z . In this report, we studied J_c as a function of magnetic field and field orientation with respect to *ab*-planes. In low magnetic field, the J_c of Sm123 thin film was almost independent of the applied angle of the field. In the case of Yb/Nd123 thin film, extremely high J_c were observed when the magnetic field was aligned parallel or perpendicular to the surface of the film. Because compositional fluctuations in RE123 thin films were observed by transmission electron microscopy, we found that the pinning centers in RE123 thin films are strongly affected by the composition in the thin films.

Index Terms—Critical current density, magnetic field, REBa₂Cu₃O_y, thin film.

I. INTRODUCTION

RECENTLY, many researchers make a great effort to develop REBa₂Cu₃O_y (RE123) coated conductors with high critical current density (J_c) in high magnetic field. We have known that the high- J_c in magnetic field is established by the introduction of artificial pinning centers (APC's) into RE123 thin film. APC's are classified into three types. The first one is 1D-APC such as dislocations, columnar defects and so on. Second, grain boundaries and twin boundaries etc. correspond to 2D-APC. At last, 3D-APC consists of participates and/or a fluctuation in a composition in a superconductor.

Manuscript received October 4, 2004.

Y. Ichino, R. Honda, M. Miura, M. Itoh, and Y. Yoshida are with the Dept. of Energy Eng. and Sci., Nagoya Univ., Furo-cho, Chikusa-ku, Nagoya 464-8603, Japan. They are also with CREST, Japan Science and Technology Agency (CREST-JST) (e-mail: ichino@nuee.nagoya-u.ac.jp).

Y. Takai is with the Dept. of Energy Eng. and Sci., Nagoya Univ., Furo-cho, Chikusa-ku, Nagoya 464-8603, Japan.

K. Matsumoto is with the Dep. of Material Sci. and Eng., Kyoto Univ., Japan. He is also with CREST-JST, Yoshida-honmachi, Sakyo-ku, Kyoto 606-8501, Japan.

M. Mukaida is with the Faculty of Eng., Yamagata Univ., Japan. He is also with CREST-JST, Yonezawa, Yamagata 992-8501, Japan.

A. Ichinose is with Central Research Institute of Electric Power Industry, Japan. He is also with CREST-JST, Yokosuka, Kanagawa 201-8511, Japan.

S. Horii is with the Dept. of Superconductivity, the Univ. of Tokyo, Japan. He is also with CREST-JST, Hongo 7-3-1, Bunkyo-ku, Tokyo 113-8656, Japan.

Digital Object Identifier 10.1109/TASC.2005.849416

To introduce APC's into RE123 thin film, we have studied a novel deposition technique and a RE123 mixed crystal thin film. The former corresponds to Low temperature growth (LTG) technique, and we reported the Sm_{1+x}Ba_{2-x}Cu₃O_y (Sm123) thin film prepared by the LTG [1]. The latter is (Yb_{1-z}Nd_z)Ba₂Cu₃O_y (Yb/Nd123) mixed crystal thin film [2]. In this work, the pinning mechanisms in these thin films were investigated by the observation of microstructure and the magnetic field (magnitude and applied angle) and temperature dependences of J_c .

II. EXPERIMENTAL PROCEDURE

A. Film Preparation and Characterization

RE123 thin film was prepared by usual pulsed laser deposition technique on MgO (100) substrates with sintered targets. The sintered targets were synthesized by conventional solid state reaction method in air. Starting materials were high purity (99.99%) RE₂O₃, BaO₂ and CuO. Appropriate amount was accurately weighed and thoroughly mixed. In the case of Sm123 target, composition of target was Sm : Ba : Cu = 1 + x : 2 - x : 3 with the ranging from $x = 0$ to 0.08, and that for Yb/Nd123 was Yb : Nd : Ba : Cu = 1 - z : z : 2 : 3 with the ranging from $z = 0$ to 0.8. The mixed powder was pressed into pellets and sintered at 800, 900 and 950°C for 12 h with an intermediate grinding and a repressing in air, respectively.

In this study, Sm123 films were prepared by so called LTG technique using PLD. The LTG technique consists of two steps as follows. The first step is to fabricate a "seed layer" with a thickness of 100 nm under the condition of high growth temperature ($\sim 830^\circ\text{C}$). As the second step, an "upper layer" with a thickness of 500 nm is deposited at low growth temperature ($\sim 730^\circ\text{C}$). More details of the LTG were described elsewhere [1].

On the other hand, Yb/Nd123 films with the thickness of 600 nm were also fabricated as well. The conditions of PLD are as follows: ArF excimer laser ($\lambda = 193$ nm); a target-substrate distance, 5 cm; a laser energy density, 1 J/cm²; a laser repetition rate, 10 Hz. We employed substrate temperatures (T_s 's) = 750 \sim 850°C. After the film was deposited, the deposition chamber was filled with pure oxygen gas of 20 Torr, and then the substrate heater was switched off and the films were rapidly cooled to room temperature.

The orientation and crystallinity in RE123 film were checked by X-ray diffraction pattern. Microstructures were observed

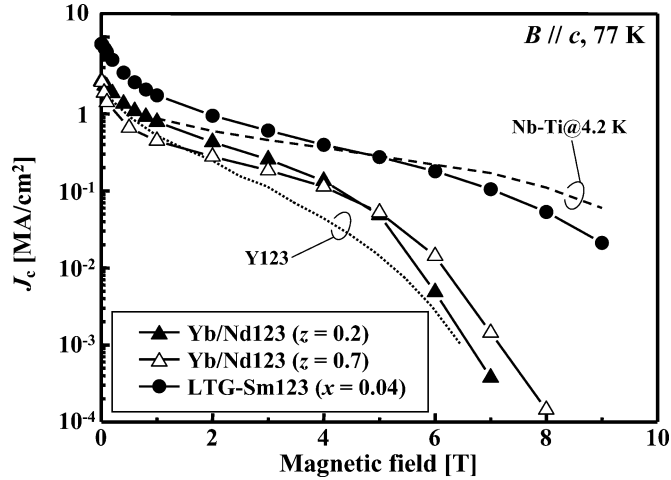


Fig. 1. J_c 's in RE123 films are plotted as a function of magnetic field applied parallel to the c -axis. The J_c in Nb-Ti wire measured at 4.2 K [4] and that in Y123 films at 77 K [3] are also represented in this figure.

using the cross sectional transmission electron microscopy (TEM). The average composition in RE123 film was evaluated by inductively coupled plasma spectroscopy. While a composition in small region of RE123 film was measured by energy dispersive X-ray spectroscopy (TEM-EDX).

B. Evaluation of Superconducting Properties

We measured superconducting properties of RE123 film with conventional dc four-probe method. Before this measurement, silver pads were deposited as electrodes on the films, and then the films were oxygenated at 350 ~ 400°C for 1~3 hours in O₂ gas flow. J_c and critical temperature (T_c) were determined by adopting an electric field criterion of 1 μ V/cm. typical T_c 's in our RE123 thin films were 91 K for LTG-Sm123, 83 K for Yb/Nd123 ($z = 0.2$) and 86 K for Yb/Nd123 ($z = 0.7$).

We have measured J_c in the presence of an applied magnetic field B as a function of the angle θ between B and c -axis of the film with J perpendicular to B . Here, a magnitude of the magnetic field was ranging from 1 to 9 T and the θ was changed from 0° ($B \parallel c$ -axis) to 90° ($B \parallel ab$ -plane).

III. RESULTS AND DISCUSSION

A. Critical Current Density in Magnetic Field

The magnetic field dependence of J_c in LTG-Sm123 thin film ($x = 0.04$) and Yb/Nd123 thin films ($z = 0.2$ and 0.7) are plotted in Fig. 1. For reference, $J_c - B$ curves in Y123 thin film [3] and Nb-Ti wire at 4.2 K [4] are also shown. From this figure, we found that the J_c at 77 K in LTG-Sm123 thin film is much higher than that in the Y123 thin film and comparable to that in Nb-Ti wire at 4.2 K. There is a crossover of the $J_c - B$ curves at 5 T in LTG-Sm123 thin film and that in Nb-Ti wire. We think in magnetic fields above 5 T, the drop of $J_c - B$ curve in LTG-Sm123 thin film comes from a thermally activated flux creep since the $J_c - B$ measurement is carried out at 77 K which is higher than 4.2 K for the Nb-Ti wire. However, the high J_c in low magnetic field for the LTG-Sm123 thin film reflects the substantial enhancement of pinning force owing to the introduction of APC's.

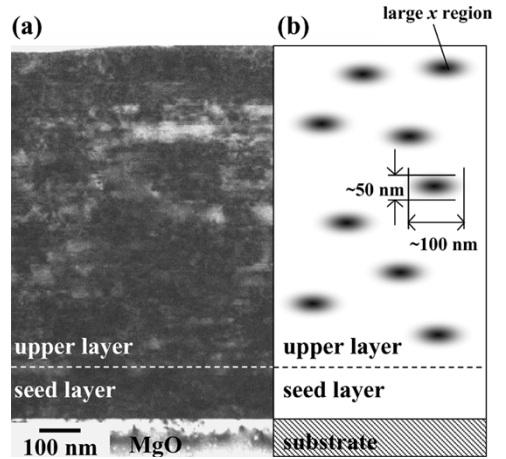


Fig. 2. Cross sectional image in LTG-Sm123 film. (a) TEM image and (b) schematic drawing of the Sm/Ba fluctuation observed by TEM-EDX. There are the refined large x regions with dimensions of ~ 50 nm \times ~ 100 nm in the upper layer. The seed layer didn't contain such large x regions.

In the case of Yb/Nd123 thin films, we investigated the effect of the mixed crystal ratio z on $J_c - B$ curves. As shown in Fig. 1, both J_c in Yb/Nd123 thin films with $z = 0.2$ and 0.7 are higher than that in Y123 thin film. A. R. Devi *et al.* fabricated Y/Dy123 mixed crystal thin film using PLD method and studied the effect of crystal defects created by stress fields on flux pinning and J_c [5]. The higher $J_c - B$ curves in Yb/Nd123 thin film imply that crystal defects originating from a lattice misfit between Yb123 and Nd123 act as APC's. Other groups also argued the improvement on the pinning force in the RE123 mixed crystal [5]–[7]. The J_c in high magnetic field in Yb/Nd123 thin film with $z = 0.7$ was higher than that with $z = 0.2$, because the T_c 's are 83 K and 86 K in Yb/Nd123 thin film with $z = 0.2$ and 0.7, respectively.

B. Microstructures in REBa₂Cu₃O_y thin films

As discussed above, RE123 thin films prepared by LTG technique and mixed crystal system showed excellent $J_c - B$ curves. To clarify pinning centers in these films, we observed cross sectional TEM images in RE123 thin films.

Fig. 2 shows the microstructure of LTG-Sm123 thin film. In Fig. 2(a), we noted the lack of precipitates and any distinctive defects in the film. In order to investigate the candidate for APC's, we measured the distribution of the composition in the film using TEM-EDX in Fig. 2(b). In this figure, a grayscale represents an amount of Sm/Ba substitution x . We found that the upper layer contains a lot of refined large x regions with dimensions of ~ 50 nm \times ~ 100 nm. It is well known that a large x in Sm123 causes decrease in T_c . Therefore, we suggest that fluxons are pinned by these refined low- T_c phases.

We also performed cross sectional TEM in an Yb/Nd123 thin film ($z = 0.2$) as shown in Fig. 3. Although we can observe columnar contrasts along the substrate normal in Fig. 3(a), their origin is not cleared. They may come from a fluctuation in a composition, a misalignment of crystallographic axes and so on. In order to clarify reasons for the improved $J_c - B$ curves, a fluctuation in a composition was measured by TEM-EDX. Fig. 3(b) shows RE fluctuation measured at the dashed line represented

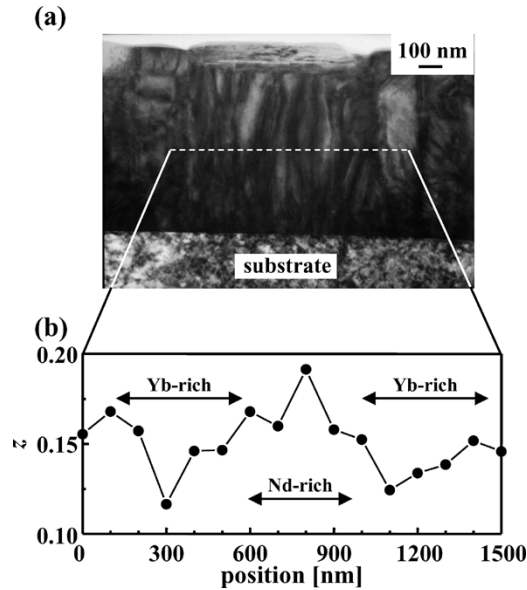


Fig. 3. Microstructure and fluctuation in composition in Yb/Nd123 thin film ($z = 0.2$). (a) represents the cross sectional TEM image and (b) is the RE fluctuation as a function of horizontal position which corresponds to the dashed line in (a).

in Fig. 3(a). Yb-rich domains and Nd-rich domains are periodically seen with a separation of 400~500 nm, but shapes of these domains have not been revealed. In the case of (Nd,Eu,Gd)123 melt processed bulk with the excellent magnetic properties, the nanoscale laminar structure have been observed by a dynamic force microscope viewed from [001] direction, and the period in this structure is comparable to the coherence length [8]. We speculate that the periodic structure in Yb/Nd123 thin film is similar to the laminar structure in the (Nd,Eu,Gd)123 bulk, although the period in the film is several hundred times larger than that in the (Nd,Eu,Gd)123 bulk.

C. Effect of Field Angle and Temperature on J_c

From the microstructures in RE123 thin films, there is a possibility that the fluctuation in the composition acts as APC's. One of the most straightforward methods to evaluate pinning effects due to APC's in RE123 thin films with some degree of spatial alignment is measuring the dependence of J_c on the angle θ between the magnetic field B and the c -axis in the films. When B is aligned with defects, any influence of defects on flux pinning can be revealed clearly as a J_c anomaly.

We present the $J_c - \theta$ curves taken at various temperatures and the several values of the magnetic field for LTG-Sm123 thin film in Fig. 4. In this figure, the vertical axis is a J_c divided by $J_c(B \parallel ab)$ which corresponds to $J_c(\theta = 90^\circ)$, and t represents the temperature T reduced by $T_c = 91$ K in 0 T, i.e. $t = 0.8, 0.85$ and 0.9 correspond to $T = 73, 77$ and 82 K, respectively. For comparison, the J_c in Y123 film on MgO is also plotted [9].

It can be seen that the $J_c - \theta$ curves at 1 T hardly depend on θ . On the other hand, at 5 T, broad J_c peaks were observed when the B was aligned parallel to the CuO planes ($\theta = 90^\circ$). Furthermore, an additional J_c peak occurs only at $t = 0.9$ and $\theta = 0^\circ$. In the case of the $J_c - \theta$ curve in Y123 thin film, a sharp J_c peak is observed when field is aligned with the CuO planes,

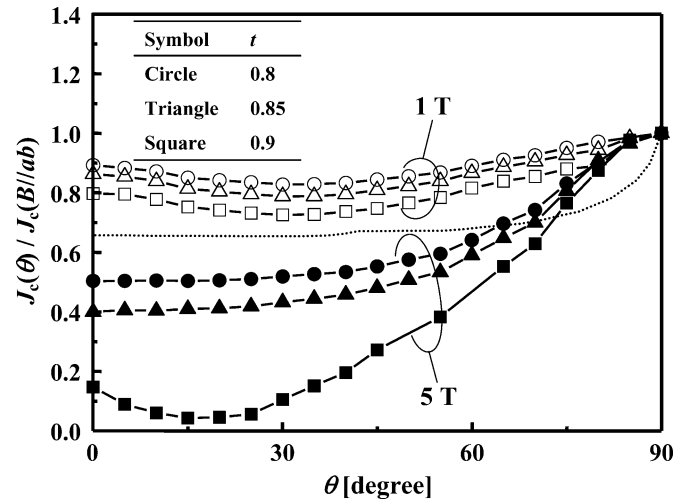


Fig. 4. Normalized J_c in LTG-Sm123 thin film at different temperatures as a function of field angle θ . Opened and filled symbols show the J_c at 1 T and 5 T, respectively. Here, t is reduced measurement temperature T by $T_c = 91$ K. The dotted line corresponds to the J_c in Y123 on MgO for comparison ($T_c = 87$ K, $T = 77$ K, 1 T) [9].

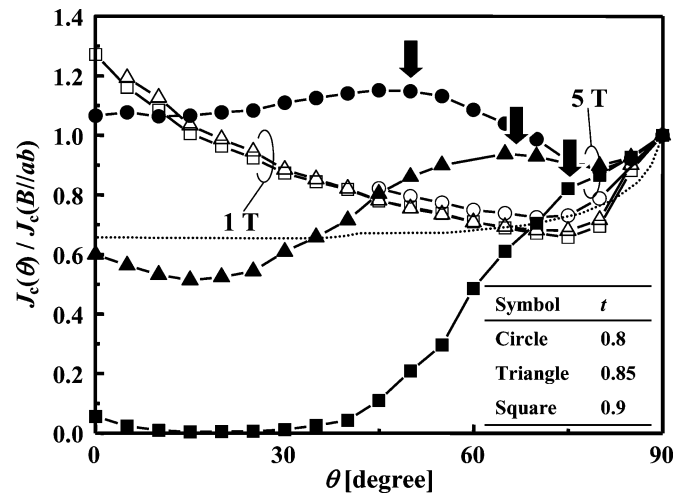


Fig. 5. Normalized J_c in Yb/Nd123 thin film ($z = 0.7$) at different temperatures as a function of field angle θ . The T_c in this film was 86 K. Opened and filled symbols show the J_c at 1 T and 5 T, respectively. Anomalous J_c peaks appeared at 5 T and were pointed out by the black arrows. The dotted line corresponds to the J_c in Y123 on MgO for comparison ($T_c = 87$ K, $T = 77$ K, 1 T) [9].

and an additional J_c peak appears at around $\theta = 0^\circ$ in some instances, for example when the B is aligned with defects correlated along the c -axis of the film such as dislocations [10], [11]. Thus, the additional J_c peak is due to correlated dislocation $\parallel c$ -axis, it is just hidden by the higher J_c values of lower angle-dependences, which the large- x regions are dominant, presumably. On the basis of both results, we suggest that these regions contribute to the isotropic $J_c - \theta$ curve, since fluxons can be pinned when B is aligned with any directions.

Next, we also present the $J_c - \theta$ curves measured at various temperatures and several values of the magnetic field for Yb/Nd123 thin film ($z = 0.7$) in Fig. 5. Here, T_c is 86 K, therefore $t = 0.8, 0.85$ and 0.9 correspond to $T = 69, 73$ and 77 K, respectively.

As seen in Fig. 5, $J_c(B \parallel c)$ at 1 T is larger than $J_c(B \parallel ab)$ independent of t . Similar results are reported in the literature [12]. Their broad J_c peaks at around $\theta = 0^\circ$ appeared in Y123 films deposited on SrTiO₃ and LaAlO₃, because the c -axis directed pinning centers such as dislocations were generated on the substrates. Although our films were deposited on MgO, our result also originates from pinning centers correlated along the c -axis. Additionally, from the TEM observation in Yb/Nd123 thin film ($z = 0.2$), there are the RE fluctuations in the film. Although the $J_c - \theta$ measurements were carried out on Yb/Nd123 thin film ($z = 0.7$), we expect a similar microstructure in the film. From the viewpoint of RE fluctuations in the film, we suggest that pinning centers correlated along the c -axis are also generated by lattice misfit between Yb-rich domain and Nd-rich domain.

Interestingly, anomalous J_c peaks appeared at 5 T and angles between 0° and 90° , and shifted to lower angles for decreasing t . We can not explain mechanisms for the appearance of the anomalous J_c peaks yet. However, there is a possibility that pinning centers introduced by the RE fluctuations affect the $J_c - \theta$ curves.

IV. CONCLUSION

We have measured J_c 's and microstructures in LTG-Sm123 ($x = 0.04$) and Yb/Nd123 thin film ($z = 0.2$ and 0.7). High J_c in magnetic field comparable to J_c in Nb-Ti wire at 4.2 K was achieved by LTG-Sm123 thin film, and $J_c - B$ curves in Yb/Nd123 thin films were higher than that in Y123 thin film. From the results both of TEM observations and $J_c - \theta$ measurements, we suggest that APC's in LTG-Sm123 thin films are the refined large x regions with dimensions of $\sim 50 \text{ nm} \times \sim 100 \text{ nm}$ and those in Yb/Nd123 thin films are the RE fluctuations with a separation of $400 \sim 500 \text{ nm}$.

REFERENCES

- [1] M. Itoh, Y. Yoshida, Y. Ichino, M. Miura, Y. Takai, and K. Matsumoto *et al.*, "Low temperature growth of high- J_c Sm_{1+x}Ba_{2-x}Cu₃O_y films," *Physica C*, vol. 412–414, pp. 833–837, 2004.
- [2] Y. Ichino, R. Honda, K. Sudoh, Y. Yoshida, K. Matsumoto, and Y. Takai *et al.*, "The advantages of YbBa₂Cu₃O_y thin films for superconducting wire application," *Physica C*, vol. 392–396, pp. 1250–1255, 2003.
- [3] V. Boffa, T. Petrison, L. Ciontea, U. Gambardella, and S. Barbanera, "Properties of in-situ laser-pulsed deposited YBCO thin films on MgO with SrTiO₃ buffer layer," *Physica C*, vol. 260, pp. 111–116, 1996.
- [4] C. Meingast and D. C. Larbalestier, "Quantitative description of a very high critical current density Nb-Ti superconductor during its final optimization strain. II. Flux pinning mechanisms," *J. Appl. Phys.*, vol. 66, pp. 5971–5983, 1989.
- [5] A. R. Devi, V. S. Bai, P. V. Patanjali, R. Pinto, N. H. Kumar, and S. K. Malik, "Enhanced critical current density due to flux pinning from lattice defects in pulsed laser ablated Y_{1-x}Dy_xBa₂Cu₃O_{7- δ} thin films," *Supercond. Sci. Technol.*, vol. 13, pp. 935–939, 2000.
- [6] M. R. Koblischka, M. Muralidhar, and M. Murakami, "Flux pinning in ternary (Nd_{0.33}Eu_{0.33}Gd_{0.33})Ba₂Cu₃O_y melt-processed superconductors," *Appl. Phys. Lett.*, vol. 73, pp. 2351–2353, 1998.
- [7] C. Cai, B. Holzapfel, J. Hanisch, L. Fernandez, and L. Schultz, "High critical current density and its field dependence in mixed rare earth (Nd, Eu, Gd)Ba₂Cu₃O_{7- δ} thin films," *Appl. Phys. Lett.*, vol. 84, pp. 377–379, 2004.
- [8] M. Muralidhar, N. Sakai, M. Nishiyama, M. Jirsa, T. Machi, and M. Murakami, "Pinning characteristics in chemically modified (Nd, Eu, Gd)-Ba-Cu-O superconductors," *Appl. Phys. Lett.*, vol. 82, pp. 943–945, 2003.
- [9] T. Horide, K. Matsumoto, K. Osamura, A. Ichinose, and M. Mukaida *et al.*, "Flux pinning properties of YBCO thin films deposited on SrTiO₃(100) and MgO(100) substrates," *Physica C*, vol. 412–414, pp. 1291–1295, 2004.
- [10] B. Roas, L. Schultz, and G. Saemann-Ischenko, "Anisotropy of the critical current density in epitaxial YBa₂Cu₃O_y films," *Phys. Rev. Lett.*, vol. 64, pp. 479–482, 1990.
- [11] A. Dfaz, L. Mechin, P. Berghuis, and J. E. Evetts, "Evidence for vortex pinning by dislocations in YBa₂Cu₃O_{7- δ} low-angle grain boundaries," *Phys. Rev. Lett.*, vol. 80, pp. 3855–3858, 1998.
- [12] H. Yamada, H. Yamasaki, K. Develos-Bagarinao, Y. Nakagawa, Y. Mawatari, and H. Obara, "Magnetic-field angle dependence of critical currents in pulsed-laser-deposited YBCO films," *Physica C*, vol. 392–396, pp. 1068–1072, 2003.